



Li intercalated Graphene on SiC(0001)

FROM 14/05/18 TO 31/07/18

CONFIDENTIALITY: NO

Author:
Marion BONHOMME
PNS

Tutors:
Dr. Stefan HEUN
Yuya Murata

Ecole nationale supérieure de physique,
électronique et matériaux, Phelma
Bat Grenoble-INP Minatec
3 Parvis Louis Néel - CS 50257
38016 Grenoble Cedex 1
Tél. : +33 4 56 52 91 00

Laboratorio NEST
Scuola Normale Superiore
Piazza San Silvestro 12
56127 Pisa - ITALY
Tel. +39 050 509480

Acknowledgements

I would first like to express my sincere gratitude to my supervisor Dr Stefan Heun for welcoming me in the lab and advising me during all the project. I would also like to thank him for reading my report and his helpful comments.

I would also like to thank Yuya Murata for his patience during all the project and for teaching me how to use the lab equipment. I would also like to thank him for his welcome and reading my report.

My sincere thanks also goes to all the lab team for their great welcome.

The National Enterprise for nanoScience and nanoTechnology (NEST)

NEST is located in Pisa in Italy. Scuola Normale Superiore, Istituto Italiano di Tecnologia, Consiglio Nazionale delle Ricerche and Scuola Superiore Sant'Anna are the four institutions which composed NEST initiative. It is a research centre specialized on issues at nanoscale. Research works are divided in three main domains: Nanophysics, Advanced Photonics and NanoBioScience.

I was integrated into Dr Stefan Heun's group. The group works on physics of low-dimensional systems. This includes the synthesis of nanostructures, manipulation of samples on the nanometer-scale and their characterization with spatially resolved spectroscopic techniques. Their recent activities are on graphene and black phosphorus.

Contents

Introduction	1
1 State of the art	2
1.1 Graphene	2
1.2 Graphene on SiC(0001)	3
1.3 Li on Graphene SiC(0001)	4
2 Experimental methods	6
2.1 Ultra High Vacuum (UHV)	6
2.2 Scanning Tunneling Microscope	7
2.3 Low Energy Electron Diffraction	8
2.4 Li evaporator	8
3 Li on SiC(0001)	9
3.1 Clean surface	9
3.2 Li deposition	10
3.3 Annealing	11
4 Results	14
4.1 Height difference between $6\sqrt{3}$ reconstruction and 1x1 reconstruction before and after annealing	14
4.1.1 Buffer Layer	14
4.1.2 Monolayer Graphene	16
4.1.3 Discussion	17
4.2 Triangles	18

4.2.1	Triangles height	18
4.2.2	Triangles orientation	20
4.2.3	Dark triangles	22
Conclusion		24
A Experimental conditions		27
A.1	Sample 1	27
A.2	Sample 2	28
B Gantt diagram		30

List of Figures

1	Schematic representation of the graphene lattice. From ref [1]	2
2	(a) SiC 6H projected on $(11\bar{2}0)$, ref [2] (b) SiC 6H with superposition of the stacking scheme, ref [2]	3
3	(a) Schematic side view of SiC (0001) with buffer layer, monolayer and bilayer graphene on the top ref [1] (b) Schematic top view of SiC of the buffer layer on SiC(0001) ref [3]	4
4	(a) Schematic representation of Li intercalation between buffer layer graphene and SiC; (b) Schematic representation of Li intercalation between buffer layer and ML graphene, between buffer layer graphene and SiC (c) Li (green dots) and C (white and grey dots), $(\sqrt{3} \times \sqrt{3})$ reconstruction, ref [4]	5
5	Image of Scanning Tunneling Microscope used for experiments	7
6	Representation of the Scanning Tunneling Microscope Ref [5]	7
7	Image of Li evaporator Ref [1]	8
8	(a) LEED pattern of pristine graphene. Electron energy: 95 eV (b) STM images of pristine graphene from $1 \times 1 \mu\text{m}^2$ scan area. Image parameters: 1V 1nA	9
9	(a) LEED pattern after 1 min of Li deposition; Electron energy: 120 eV (b) STM image with $500 \times 500 \text{ nm}^2$ scan area; image parameters: 800mV 1nA (c) STM image with $20 \times 20 \text{ nm}^2$ scan area; image parameters: 500mV 0.6nA	10
10	(a) LEED pattern after 3 min of Li deposition; Electron energy: 95 eV (b) STM image with $20 \times 20 \text{ nm}^2$ scan area; image parameters: -600mV -170pA	11
11	(a) LEED pattern after 33 min of Li deposition; Electron energy: 146 eV (b) STM image with $20 \times 20 \text{ nm}^2$ scan area; image parameters: 1V 1nA	11

12	LEED patterns (a) Electron energy: 142 eV (b) Electron energy: 139 eV (c) Electron energy: 95 eV (d) Electron energy: 95 eV (e) Electron energy: 121 eV (f) Electron energy: 95 eV	12
13	STM images(a) 5x5 nm ² scan area; Image parameters: 600mV 170pA (b) 100x100 nm ² scan area; Image parameters: 400mV 170pA (c) 100x100 nm ² scan area; Image parameters: 600mV 170pA (d) 100x100 nm ² scan area; Image parameters: 1V 170pA (e) 100x100 nm ² scan area; Image parameters: 2V 170pA (f) 100x100 nm ² scan area; Image parameters: 1V 200pA . . .	13
14	(a) STM image; 30x30 nm ² scan area; image parameters: 1V 170 pA (b) Histogram: the height difference between 1x1 and 6√3 is 2.0 Å	15
15	Height difference between 1x1 and 6√3 area on buffer layer graphene before and after annealing	15
16	Height difference between 1x1 and 6√3 area on ML graphene before and after annealing	16
17	Schematic representation of the Li distribution under buffer layer graphene (a) before annealing (b) after annealing	17
18	Schematic representation of the Li distribution for the case of monolayer graphene (a) before annealing (b) after annealing	17
19	STM images: 100x100 nm ² scan area, (a) before Li deposition, image parameters: 1V 1nA, (b) after annealing up to 800°C, image parameters: 2V 170pA	18
20	STM images: 50x50 nm ² scan area; image parameters: -1V -170 pA (b) height of triangle with 1x1 periodicity on the top	19
21	(a) STM image: 20x20 nm ² scan area; image parameters: -1V -170 pA (b) height of triangle with 6√3 periodicity on the top	19
22	STM images: 20x20 nm ² scan area; image parameters: -1V -170 pA (b) height of the dark triangle	19
23	Image parameters of figure (a), (b), (c): 300mV 170pA (a) 500x500 nm ² scan area (b) zoom on left part of figure (a) 55x55 nm ² scan area; (c) zoom on the right part of figure (a) 100x100 nm ² scan area; (d) 215x215 nm ² scan area; Image parameters: 1V 1nA (e) cross section along blue line in (d) . .	20
24	Schema of one step of SiC substrate where geometry of the substrate on the surface is (a) the same (b) opposite	21
25	Triangle orientation between two steps at different positions	22

26	(a) 50x50 nm ² scan area; Image parameters of figure: 1V 170pA, (b) 20x20 nm ² scan area, Image parameters: 1V 170pA, (c) 10x10 nm ² scan area; Image parameters: -1V -170pA	22
27	(a) 5x5 nm ² scan area; Image parameters of figure: -1V -170pA, (b) image (a) after correct distortion, (c) model in which there is a rotation of 0.73° between graphene (green circles) and SiC (blue circles)	23

List of Tables

4.1	Orientation of bright triangles according to the height difference of SiC steps	21
A.1	Experimental conditions of sample's degassing	27
A.2	Experimental conditions for Li deposition; Parameters: 4.5 V 6.9 A	27
A.3	Annealing parameters	28
A.4	Experimental conditions of sample's degassing	28
A.5	Experimental conditions for Li deposition; Parameters: 4.5 V 6.9 A	28
A.6	Annealing parameters	29

List of Acronyms

BL	<i>Buffer Layer</i>
EMLG	<i>Epitaxial MonoLayer Graphene</i>
LEED	<i>Low Energy Electron Diffraction</i>
Li	<i>Lithium</i>
ML	<i>Monolayer</i>
Pyro	<i>Pyrometer</i>
QFBLG	<i>Quasi-Free-standing BiLayer Graphene</i>
QFMLG	<i>Quasi-Free-standing MonoLayer Graphene</i>
STM	<i>Scanning Tunneling Microscope</i>
Thermo	<i>Thermocouple</i>

Introduction

Graphene is a carbon sheet arranged in honeycomb structure and one-atom thick. Graphene was exfoliated for the first time in 2004 by A. Geim and K. Novoselov. Since then, graphene is one of the most studied material because of its extraordinary properties like a very good electrical and thermal conductivity, high charge mobility, low optical absorbance .

Scientists studied atoms which decorated graphene like Li, Na, Co ... Our choice is to study Li on graphene because of its different applications such as battery technology [6], hydrogen storage [7] and superconductivity[8]. The group of Dr. Stefan Heun, at CNR-Nano in Pisa has recently performed the first work in which the interaction between Li atoms and epitaxial monolayer graphene (EMLG) on SiC(0001) was studied in details by scanning tunneling microscopy (STM)[9].

The goal of this work is to investigate the Li intercalation / deintercalation dynamics in greater detail. In order to do this, the functionalization of graphene on Silicon Carbide(SiC) by Lithium (Li) is studied by using Scanning Tunneling Microscope (STM) and Low Energy Electron Diffraction (LEED).

This report is divided in four chapters:

- chapter 1 will present the state of art;
- chapter 2 will present experimental methods that have been used for experiments;
- chapter 3 will present the intercalation of Lithium on SiC;
- chapter 4 will presents the results;
- Finally, we shall present a conclusion.

Chapter 1

State of the art

This chapter will present an overview of the state of the art about graphene, graphene on SiC(0001) and the intercalation of Li on SiC(0001).

1.1 Graphene

Graphene is a 2D material of one atom thick. It is arranged in a honeycomb configuration as shown in figure 1. The distance between two carbon atoms is 1.42 \AA . The graphene unit cell contains two carbon atoms labeled A and B (figure 1) and formed by two vectors \vec{a}_1 and \vec{a}_2 such that $a_1=a_2=2.46 \text{ \AA}$.

Experimentally, it was exfoliated in 2004 by A. Geim and K. Novoselov. Now, we will present how to made graphene.

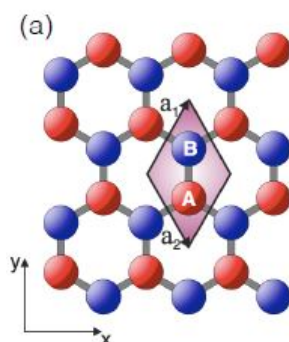


Figure 1: Schematic representation of the graphene lattice. From ref [1]

1.2 Graphene on SiC(0001)

In our sample, to obtain graphene, silicon carbide (SiC) wafer is used.

The polytype used is 6H as shown figure 2a which is an hexagonal form. The structure is ABCACB. The sequence $A \rightarrow B \rightarrow C \rightarrow A$ means that there is a translation of $(1/3 \ 2/3 \ 1/6)$ vector represented by (+) in figure 2b. The sequence $A \rightarrow C \rightarrow B \rightarrow A$ means that there is a translation of $(2/3 \ 1/3 \ 1/6)$ vector represented by (-) in figure 2b. So the sequence ABCACB can be represented as (+++- -). Thus, every three layers, there is a change between (+) and (-) configuration.

To obtain layers of graphene, SiC substrate is heated in Argon atmosphere. Indeed, by heating, silicon atoms leave by sublimation and carbon atoms that remain rearrange on the surface.

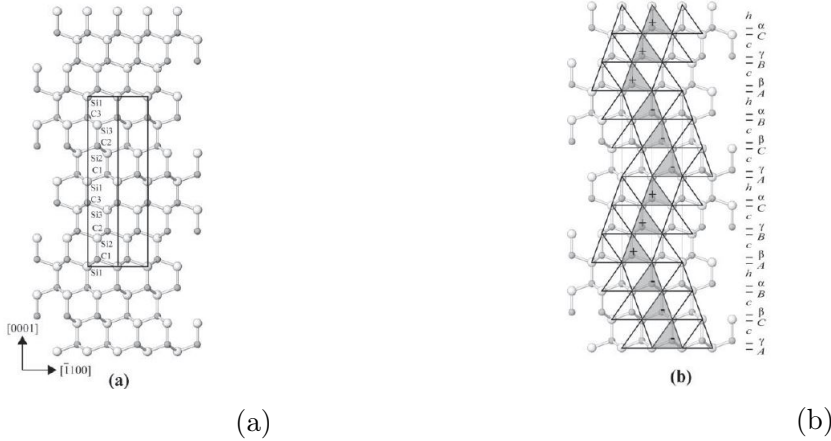


Figure 2: (a) SiC 6H projected on $(11\bar{2}0)$, ref [2] (b) SiC 6H with superposition of the stacking scheme, ref [2]

The different layers of graphene above SiC substrate have different properties depending of the link between the layer and the substrate. So they are named differently as shown in figure 3a. The first carbon layer above SiC substrate is called buffer layer and the height difference between buffer layer and substrate is around 2.3\AA [10]. Because of the difference of lattice constant between graphene and SiC, a periodicity named $(6\sqrt{3}\times 6\sqrt{3})R30^\circ$ is obtained as shown in figure 3b. There is a partial sp^3 hybridization of the buffer layer due to chemical bonds between almost 30 % of the C atoms and the dangling bonds of the Si surface atoms as represented in figure 3a.[1]

The layer above buffer layer graphene is called monolayer graphene (ML) and they interact by Van der Waals forces. This two layers are spaced from 3.6\AA .

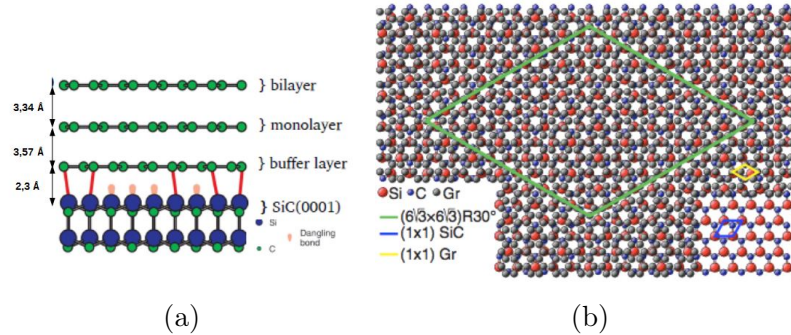


Figure 3: (a) Schematic side view of SiC (0001) with buffer layer, monolayer and bilayer graphene on the top ref [1] (b) Schematic top view of SiC of the buffer layer on SiC(0001) ref [3]

After studying graphene, we will see Li intercalation on graphene.

1.3 Li on Graphene SiC(0001)

Lithium is an alkali metal that is with a single valence electron.

Li is deposited thanks to an evaporator. First, Li atoms intercalate between SiC substrate and buffer layer graphene [9] as shown figure 4a. In this case, the Moiré pattern disappear because the SiC bonds between buffer layer and the substrate have been broken by Li intercalation. This detach the buffer layer from the substrate and the buffer layer becomes quasi free.

If more Li is deposited on monolayer graphene, Li goes between buffer layer and monolayer graphene as shown figure 4b. In this case, $(\sqrt{3} \times \sqrt{3})$ reconstruction appears as represented in figure 4c.

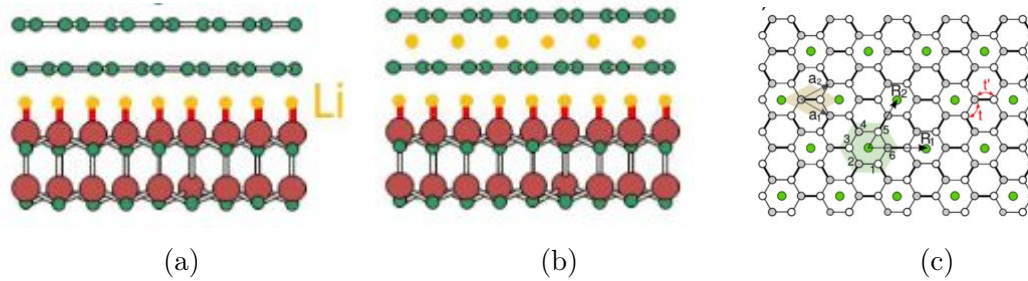


Figure 4: (a) Schematic representation of Li intercalation between buffer layer graphene and SiC; (b) Schematic representation of Li intercalation between buffer layer and ML graphene, between buffer layer graphene and SiC (c) Li (green dots) and C (white and grey dots), $(\sqrt{3} \times \sqrt{3})$ reconstruction, ref [4]

Now, after studying the theory of graphene and Li intercalation on graphene, the next part will present the experimental methods used for experiments.

Chapter 2

Experimental methods

This chapter will present the experimental methods used for experiments.

2.1 Ultra High Vacuum (UHV)

Contrary to graphene, Li is not stable in air. To avoid oxidation or any undesirable reaction of Li and so to obtain images with atomic resolution is necessary to work in Ultra High Vacuum conditions that is around 10^{-11} mbar. To reach this pressure, instrumentation resistant to this pressure is required.

The instrumentation is divided in three parts as shown figure 5 : the load lock chamber, the preparation chamber and the STM chamber. The load lock chamber is used to insert and remove samples. The pressure can be until 10^{-8} mbar. Then, the preparation chamber is used to do experiment on the sample like deposit lithium, heat the sample, do LEED . . . Pressure in this chamber is around 10^{-10} mbar. Then the STM chamber is the chamber with the Scanning Tunneling Microscope and the pressure is around 10^{-11} mbar. To obtain and keep these pressures, different pumps are necessary.

- Scroll pumps: These pumps bring down the pressure from atmospheric pressure (10^3 mbar) to 10^{-2} - 10^{-3} mbar.
- Turbomolecular pumps: These pumps is made to decrease the pressure from 10^{-2} mbar to 10^{-8} mbar. The principle is to transfer momentum to the molecule by collisions with the rotor. Then, molecules goes to into the gas transfer holes in the stator.
- Ion pumps: These pumps start around 10^{-3} mbar and are used for reach 10^{-11} mbar. The principle is to ionize molecules thanks to a strong magnetic field. Then, the molecules are accelerated with an electric field and captured by an electrode.

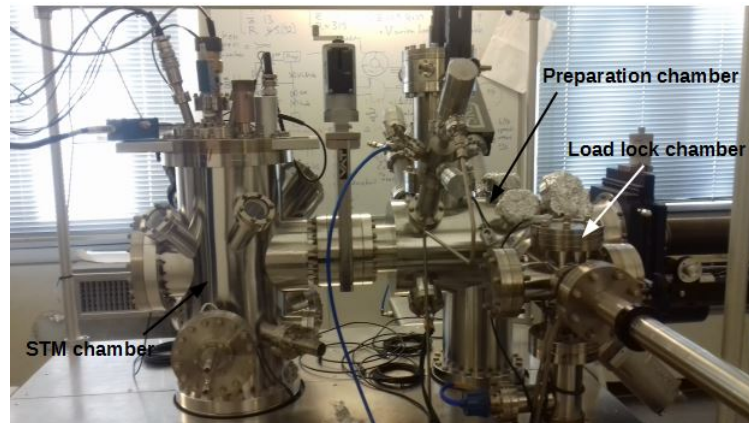


Figure 5: Image of Scanning Tunneling Microscope used for experiments

2.2 Scanning Tunneling Microscope

The Scanning Tunneling Microscope (STM) was invented by two IBM researchers, Gerd Binnig and Heinrich Rohrer in 1981. STM is used to characterize surfaces. This microscope is based on the Tunnel Effect. The figure 6 is a schematic representation of the

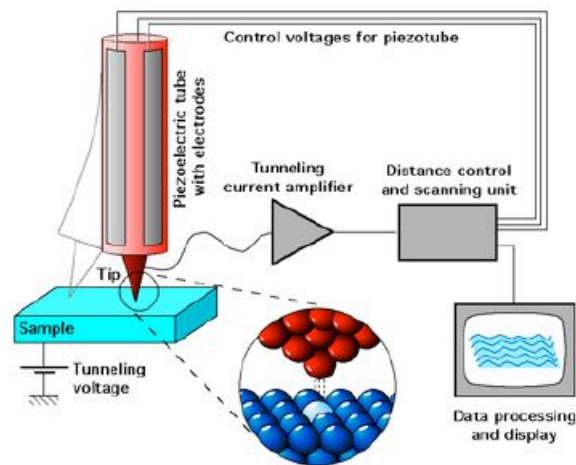


Figure 6: Representation of the Scanning Tunneling Microscope Ref [5]

STM. A tip made of tungsten is approached close to the surface thanks to piezoelectric tube. A bias voltage is applied between the tip and the sample which induces an electrical current (tunneling current) between the tip and the surface of the sample. This current is amplified by a current amplifier as shown figure 6. Then, the current is maintained constant by moving the tip in z direction thanks to piezoelectric tubes. It is the constant current mode. So, as the tip scans all the surface, an image is obtained which shows the xy plane but also the height analysis in z direction. Indeed, the bright areas in the STM

image are the high z values while the dark areas are the low z values.

Then, resolution of this microscope can reach until 0.1 \AA . But to achieve a good resolution, it is necessary to avoid as much as possible vibrations and noise. That is why STM is placed in a floating table to avoid vibrations caused by external environment. The experiments are also made in UHV conditions (as explain chapter 2.1). So, STM is a powerful tool to analyze and characterize surface in xy plane and also in z direction.

2.3 Low Energy Electron Diffraction

Low Energy Electron diffraction (LEED) provides information on symmetries of the surface. LEED is based on the wave particle duality. A collimated electron beam beats the sample surface which produces for a cristalline sample diffracted electrons. This electrons are observed as spots on a screen. The electron energy is typically between 20 eV and 200 eV resulting in Broglie wavelength in the order of inter atomic distances ($1\text{-}2 \text{ \AA}$).

2.4 Li evaporator

To deposit Lithium on the sample, a Li evaporator as shown figure 7 is inserted in the preparation chamber. The evaporator is composed by a support made with UHV-resistant materials and a Lithium dispenser. The mixture in the dispenser is not only Li but a mixture of an alkali metal chromate Li_2CrO_4 with a reducing agent. To release Li, dispenser must be degas in UHV conditions.

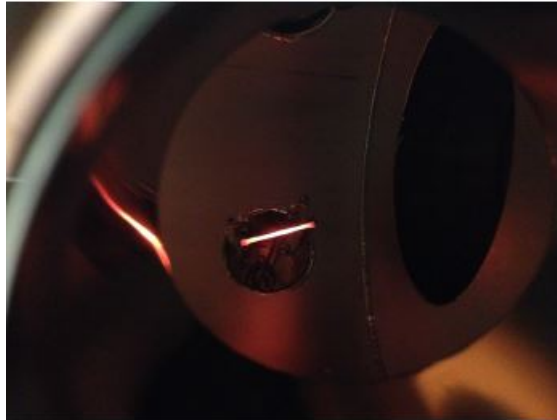


Figure 7: Image of Li evaporator Ref [1]

After studying experimental methods, we will present the results of Li deposition on SiC.

Chapter 3

Li on SiC(0001)

In this chapter, we shall present our results about the deposition of Li on graphene on SiC and results after heating the sample.

3.1 Clean surface

The sample is composed of graphene which was grown on 6H SiC substrate. Before starting Li deposition, a characterization of samples by LEED and STM is done.

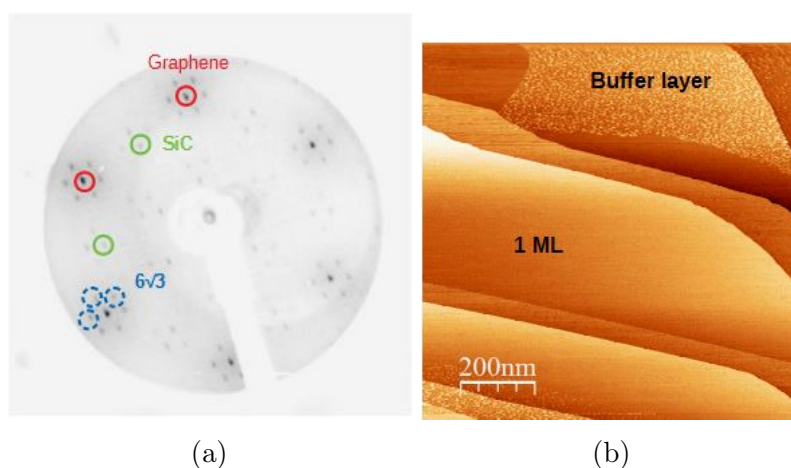


Figure 8: (a) LEED pattern of pristine graphene. Electron energy: 95 eV (b) STM images of pristine graphene from $1 \times 1 \mu\text{m}^2$ scan area. Image parameters: 1V 1nA

LEED pattern of the sample figure 8a shows three different spots: in green, the SiC spots due to the substrate, in red graphene spots and in blue the $6\sqrt{3}$ spots.

STM image figure 8b presents terraces because the SiC substrate is not cut along (0001)

plane. The height between two terraces is a multiple of 0.25 nm which is the height of a SiC step [11].

STM image in figure 8b shows different types of structure: buffer layer graphene and monolayer graphene. Buffer layer area is recognizable thanks to spots contrary to monolayer graphene area which is a flat region.

After studying STM images, it can be concluded that sample are composed around 95% of monolayer and 5% of buffer layer graphene.

3.2 Li deposition

After characterization of the sample, Li was deposited and the sample was observed by LEED and STM.

After 1 min of Li deposition, the LEED pattern in figure 9a does not show significant differences with the LEED pattern without Li deposition (figure 8a). STM image in figure 9b shows some "dark" spots. The figure 9c is a zoom of the figure 9b which shows that the Moiré pattern is interrupted in some points. This is a proof that Li intercalate at the interface and break the Si-C covalent bonds.

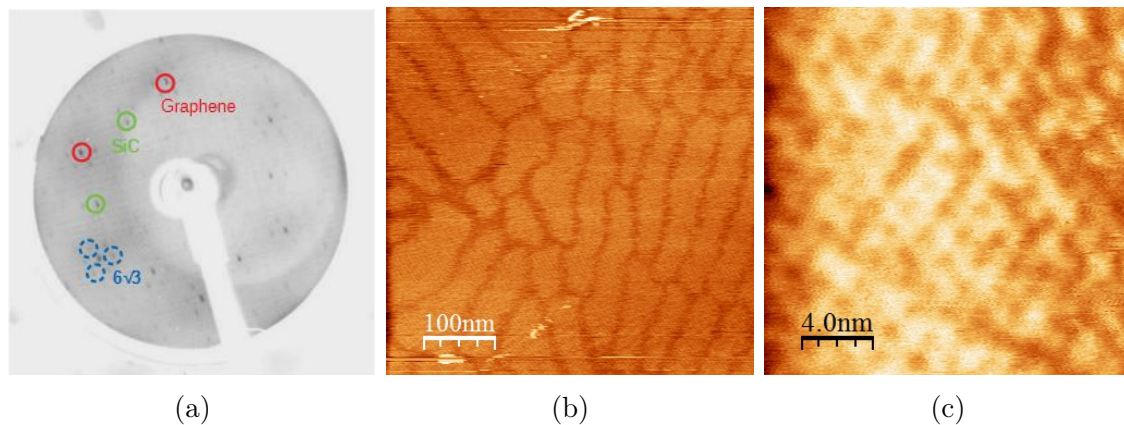


Figure 9: (a) LEED pattern after 1 min of Li deposition; Electron energy: 120 eV (b) STM image with $500 \times 500 \text{ nm}^2$ scan area; image parameters: 800mV 1nA (c) STM image with $20 \times 20 \text{ nm}^2$ scan area; image parameters: 500mV 0.6nA

After 3min of Li deposition, LEED pattern shows no difference but STM image in figure 10b shows some flat regions without $6\sqrt{3}$ reconstruction. These regions are brighter so this means that these regions are higher. The fact that $6\sqrt{3}$ periodicity disappear means that Si-C bonds at the interface between substrate and buffer layer have been broken. We can conclude that Li intercalate below graphene surface and break the SiC bonds.

After 33 min of Li deposition, $6\sqrt{3}$ spots in LEED pattern (figure 11a) disappear but new spots in yellow appear which are placed on $\sqrt{3}$ position. STM images confirm the

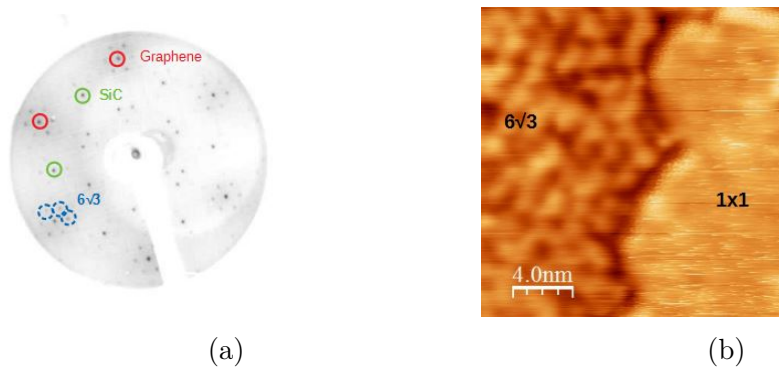


Figure 10: (a) LEED pattern after 3 min of Li deposition; Electron energy: 95 eV (b) STM image with $20 \times 20 \text{ nm}^2$ scan area; image parameters: -600mV -170pA

absence of $6\sqrt{3}$ reconstruction. This means that Li intercalates under graphene, therefore buffer layer is completely detached from the substrate. A zoom on the flat area in figure 11b shows a $\sqrt{3}$ reconstruction. This reconstruction means that Li intercalate between two layers of graphene.[4]

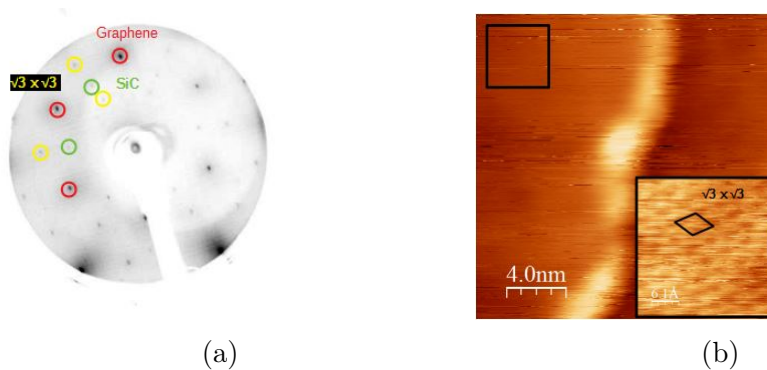


Figure 11: (a) LEED pattern after 33 min of Li deposition; Electron energy: 146 eV (b) STM image with $20 \times 20 \text{ nm}^2$ scan area; image parameters: 1V 1nA

3.3 Annealing

After Li deposition, sample is heated step by step to understand how the surface changes in response to annealing. The sample is heated from 150°C up to 900°C . After each annealing, LEED and STM were performed at room temperature.

LEED patterns in figure 12 show that there is no $\sqrt{3}$ reconstruction and the $6\sqrt{3}$ reconstruction reappear beyond 400°C . In addition, LEED patterns show that the heating makes $6\sqrt{3}$ spots brighter, which means that $6\sqrt{3}$ areas are larger and Li is desorpted.

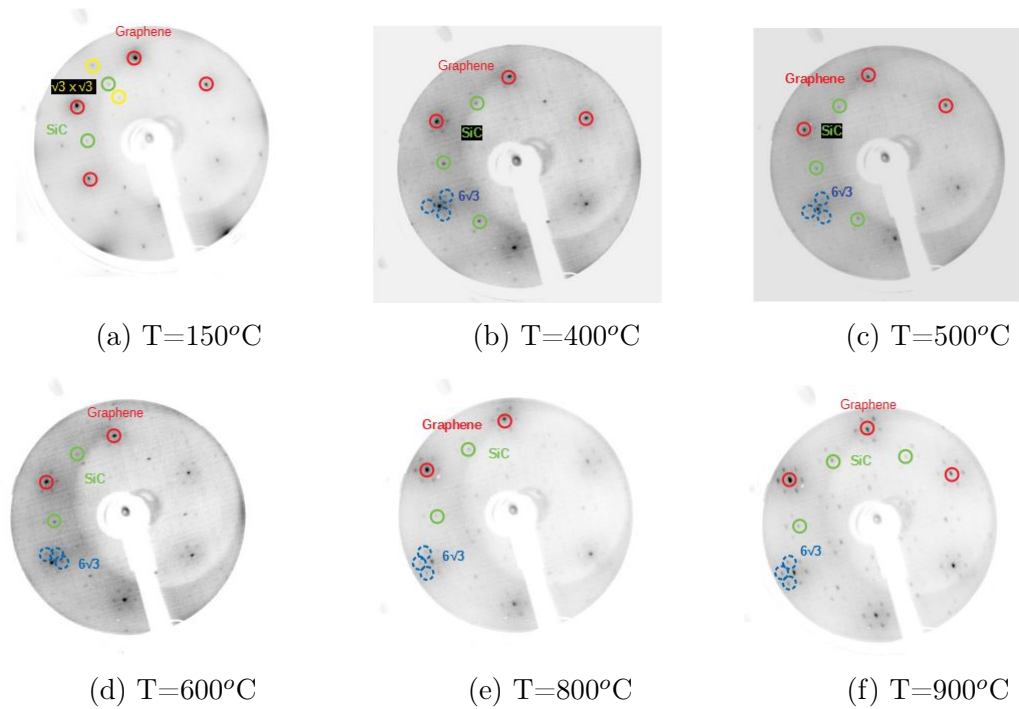


Figure 12: LEED patterns (a) Electron energy: 142 eV (b) Electron energy: 139 eV (c) Electron energy: 95 eV (d) Electron energy: 95 eV (e) Electron energy: 121 eV (f) Electron energy: 95 eV

STM images in figure 13 show that the surface changes when annealing. Above 400C, STM image in figure 13b shows Moiré on the surface. This is a proof that Li starts to desorpt. Large bright islands with 1x1 reconstruction are visible. When the temperature raises, the size of islands decreases. Above 800°C, STM image in figure 13e shows different islands. These islands are smaller and triangle-shaped. We also see the Moiré reconstruction on the top of some triangles.

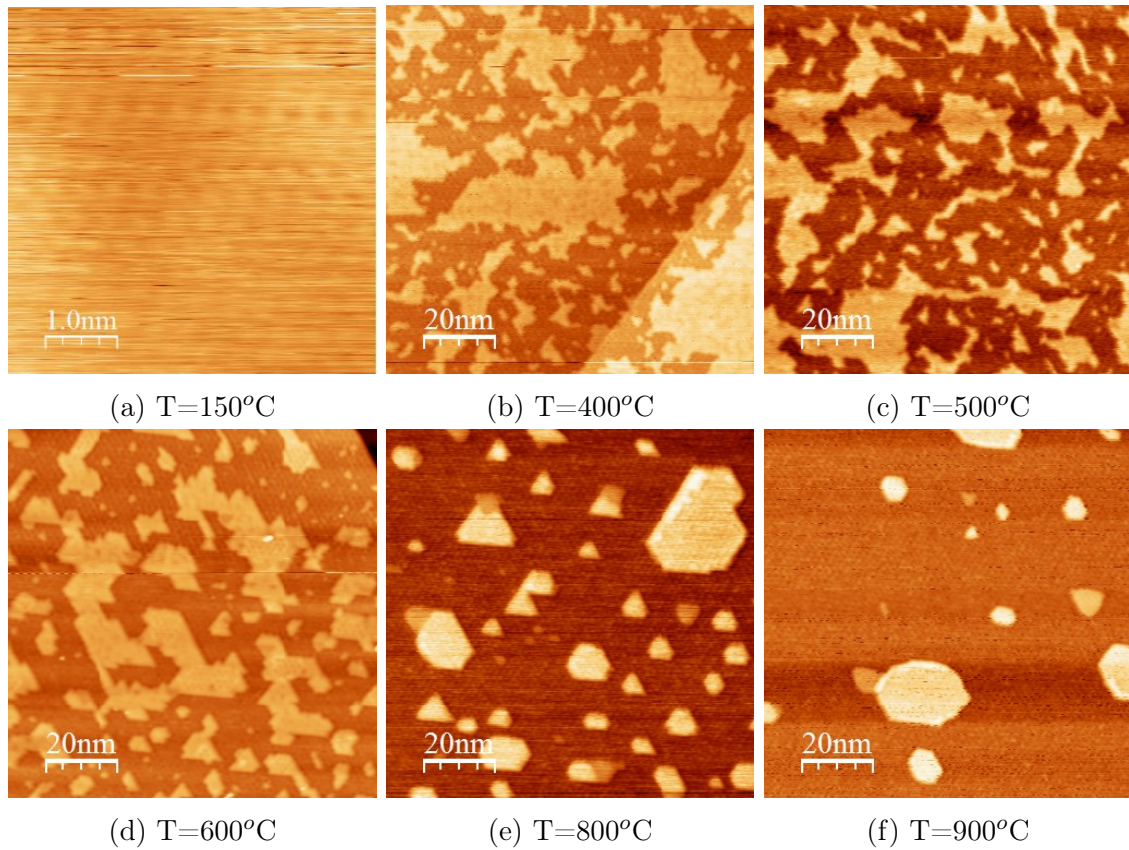


Figure 13: STM images (a) 5x5 nm² scan area; Image parameters: 600mV 170pA (b) 100x100 nm² scan area; Image parameters: 400mV 170pA (c) 100x100 nm² scan area; Image parameters: 600mV 170pA (d) 100x100 nm² scan area; Image parameters: 1V 170pA (e) 100x100 nm² scan area; Image parameters: 2V 170pA (f) 100x100 nm² scan area; Image parameters: 1V 200pA

Chapter 4

Results

In this chapter, we focus on two points: the height difference between $6\sqrt{3}$ reconstruction and 1×1 reconstruction before and after annealing and the nature of the triangles observed after heating above 800°C .

4.1 Height difference between $6\sqrt{3}$ reconstruction and 1×1 reconstruction before and after annealing

From literature [1], we know that there is a height difference between $6\sqrt{3}$ and 1×1 reconstruction before and after annealing. The goal of our experiment is to confirm and try to explain this difference. To that end, several images of the boundary between 1×1 area and $6\sqrt{3}$ area at different voltages and different positions have been taken. to prove that the difference is not a fact due to the tip conditions. In addition, two situations are studied: the case of buffer layer graphene and the case of monolayer graphene.

4.1.1 Buffer Layer

First, the case of buffer layer is studied. Several STM images are taken as shown in figure 14a. To measure the height difference, WSxM software and qtipolt are used. Thanks to WSxM software, an STM image is analyzed and as shown in figure 14b, an histogram is made which represents the number of pixels function of the height. The height difference between two areas is obtained using this histogram. Different images at different positions and voltage are analyzed with this technique. The figure 15 summarizes the results.

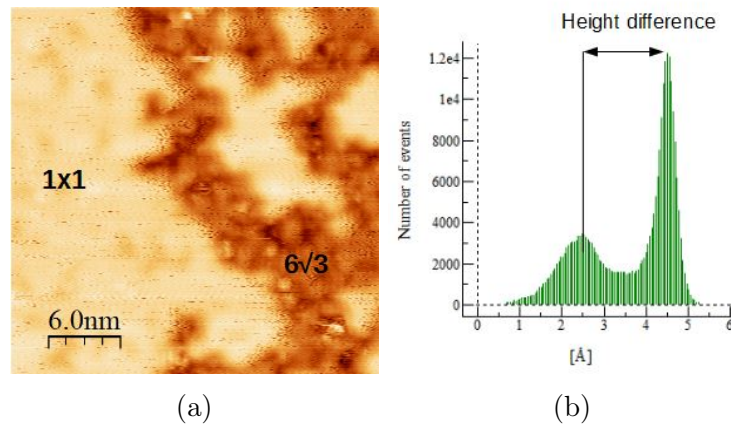


Figure 14: (a) STM image; 30×30 nm² scan area; image parameters: 1V 170 pA (b) Histogram: the height difference between 1×1 and $6\sqrt{3}$ is 2.0 \AA

Figure 15 shows that the height difference is independent of the voltage applied. The height difference between 1×1 area and $6\sqrt{3}$ area is $2.6 \pm 0.4 \text{ \AA}$ before annealing and $2.0 \pm 0.4 \text{ \AA}$ after annealing. We can conclude that taking into account error bars, there is no significant distinction on the height difference due to annealing.

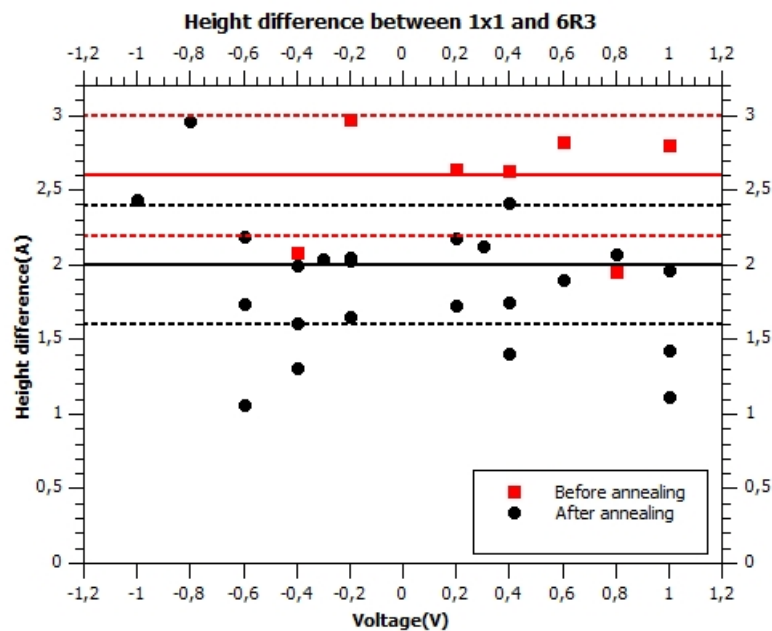


Figure 15: Height difference between 1×1 and $6\sqrt{3}$ area on buffer layer graphene before and after annealing

4.1.2 Monolayer Graphene

The second case is the Li distribution under monolayer graphene. The same protocol is made. Results are summarized in figure 16. Contrary to the case of buffer layer graphene, the height difference between 1×1 and $6\sqrt{3}$ area is clearly different before and after annealing. Indeed, the height difference before annealing is $1.0 \pm 0.3 \text{ \AA}$ whereas the height difference after annealing is $2.2 \pm 0.2 \text{ \AA}$.

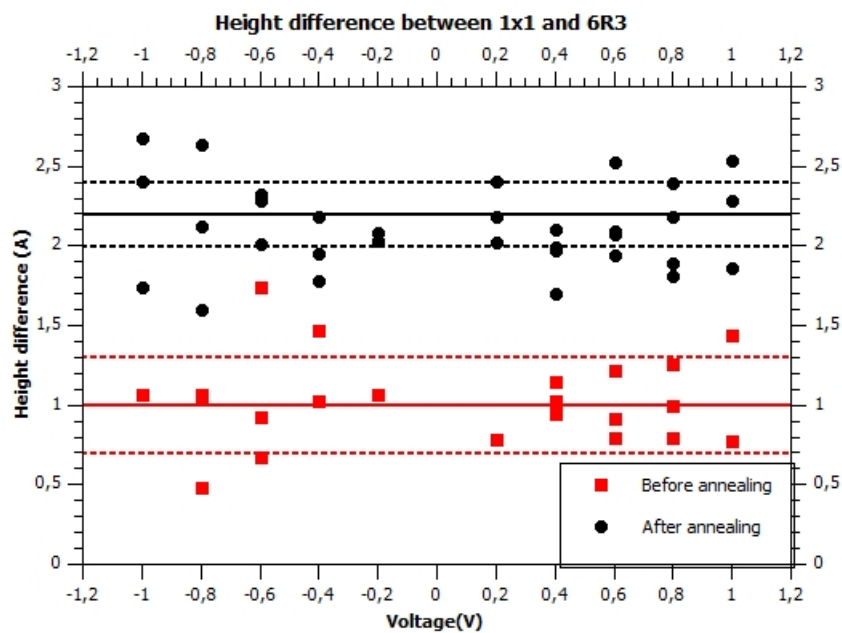


Figure 16: Height difference between 1×1 and $6\sqrt{3}$ area on ML graphene before and after annealing

4.1.3 Discussion

Now, we will discuss the results obtained for buffer layer and monolayer cases.

Figure 17 is a schematic representation of Li distribution under buffer layer graphene. The height difference between 1×1 and $6\sqrt{3}$ reconstruction is similar before and after annealing taking into consideration the measurement errors. As the height difference between SiC substrate and buffer layer is 2.3 \AA [10], we can extract the height between graphene layer and Si atoms of the substrate which is between 4.3 \AA and 4.9 \AA . These heights are consistent with the value of 4.41 \AA calculated by I. Deretzis and A. La Magna in [12].

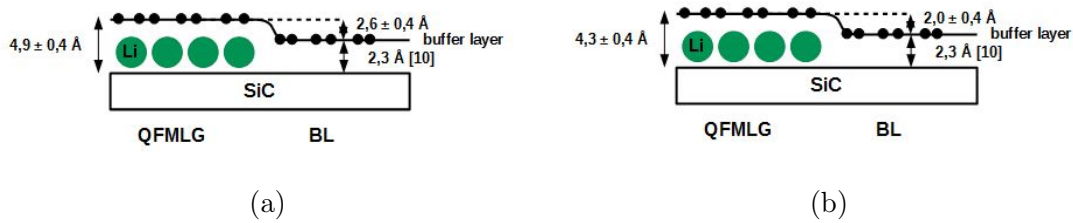


Figure 17: Schematic representation of the Li distribution under buffer layer graphene (a) before annealing (b) after annealing

Figure 18 summarize heights before and after annealing in ML case. Combining experimental values and data in reference [10], the height difference between monolayer graphene and SiC substrate is $6.9 \pm 0.3 \text{ \AA}$ before annealing and $8.1 \pm 0.2 \text{ \AA}$ after annealing.

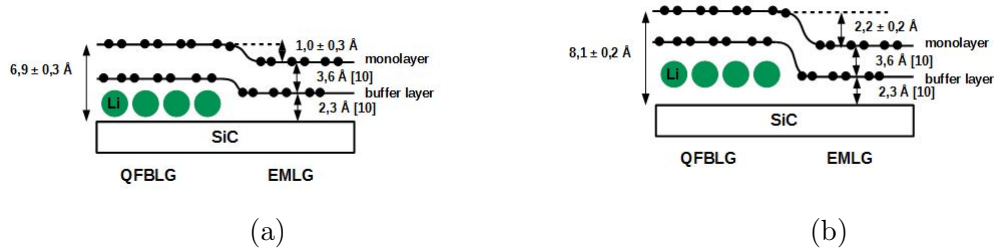


Figure 18: Schematic representation of the Li distribution for the case of monolayer graphene (a) before annealing (b) after annealing

The first conclusion is a layer of graphene above buffer layer is necessary to have a difference between before annealing and after annealing. Moreover, before annealing we deposited Li until seeing $\sqrt{3}$ reconstruction, which means that there were Li between buffer layer and monolayer graphene. Thus, an explanation of the height difference could be that Li between buffer layer and monolayer graphene do not desorpt by heating but go between SiC substrate and buffer layer graphene. This explanation is consistent with calculations made by N. Caffrey and L. Johansson [4]

4.2 Triangles

After Li deposition and annealing up to 800°C, we saw some islands triangle-shaped (figure 19b), which are not present before Li deposition as shown in figure 19a. Thus we can conclude that these islands are due to Li deposition. Besides, in figure 19b, three kinds of triangles are distinguishable: "dark triangles", triangles with 1x1 periodicity on the surface and triangles with $6\sqrt{3}$ periodicity. So, in this part, we will study more precisely these islands, particularly the height of these triangles, their orientation and the nature of the dark triangles.

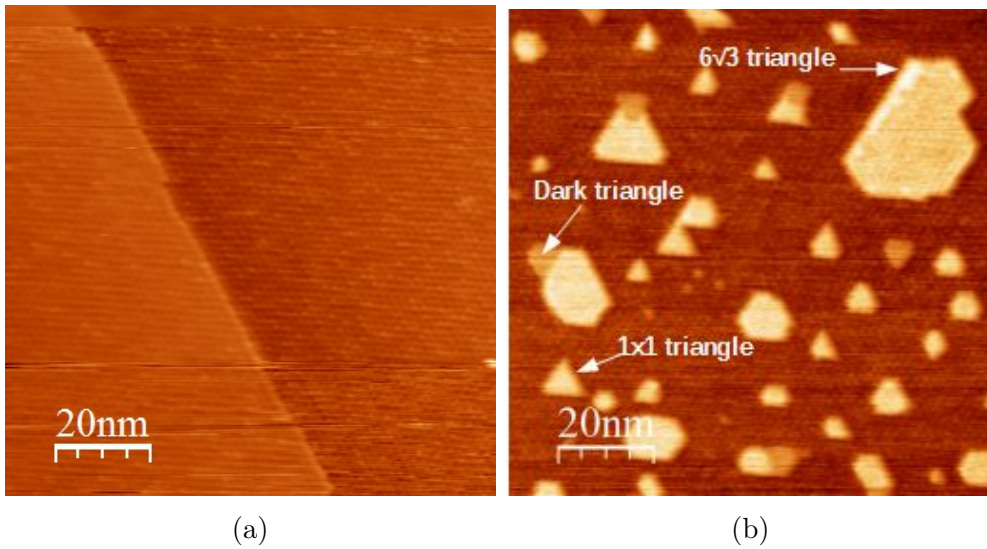


Figure 19: STM images: 100x100 nm² scan area, (a) before Li deposition, image parameters: 1V 1nA, (b) after annealing up to 800°C, image parameters: 2V 170pA

4.2.1 Triangles height

These three different triangles are present on the surface of both buffer layer graphene and monolayer graphene so these islands are independent of the number of graphene layers.

One type of these triangles is triangle with 1x1 periodicity on the top. The height difference between monolayer graphene and triangle is $2.3 \pm 0.1 \text{ \AA}$ as shown in figure 20b.

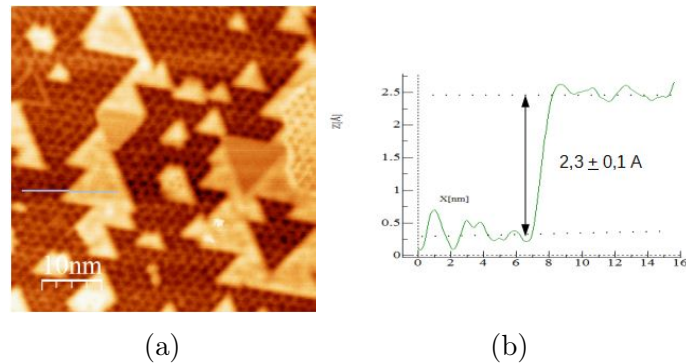


Figure 20: STM images: $50 \times 50 \text{ nm}^2$ scan area; image parameters: -1V -170 pA (b) height of triangle with 1×1 periodicity on the top

The height difference between monolayer graphene and triangle with $6\sqrt{3}$ periodicity is $2.5 \pm 0.2 \text{ \AA}$ as shown in figure 21b.

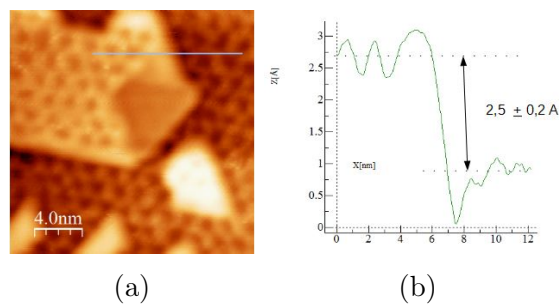


Figure 21: (a) STM image: $20 \times 20 \text{ nm}^2$ scan area; image parameters: -1V -170 pA (b) height of triangle with $6\sqrt{3}$ periodicity on the top

The height difference between monolayer graphene and dark triangle is $1.4 \pm 0.3 \text{ \AA}$ as shown in figure 22b.

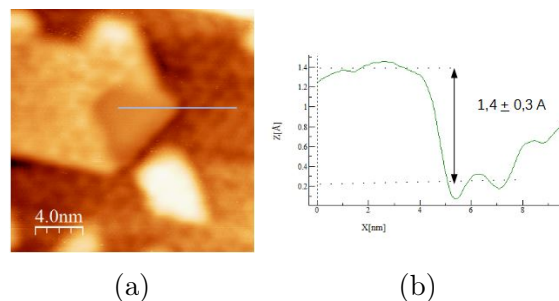


Figure 22: STM images: $20 \times 20 \text{ nm}^2$ scan area; image parameters: -1V -170 pA (b) height of the dark triangle

4.2.2 Triangles orientation

Figure 20a shows that the bright triangles (triangles with 1×1 periodicity on the top and triangles with $6\sqrt{3}$ periodicity on the top) are always in the same direction and dark triangles are always in the opposite direction of the bright triangles.

Besides, STM image in figure 23a shows that the left part is brighter than the right part. The height difference between the left and the right part is 1 nm equivalent to four steps of SiC. Furthermore, the bright triangles point in opposite directions between two steps as shown in figure 23b and figure 23c.

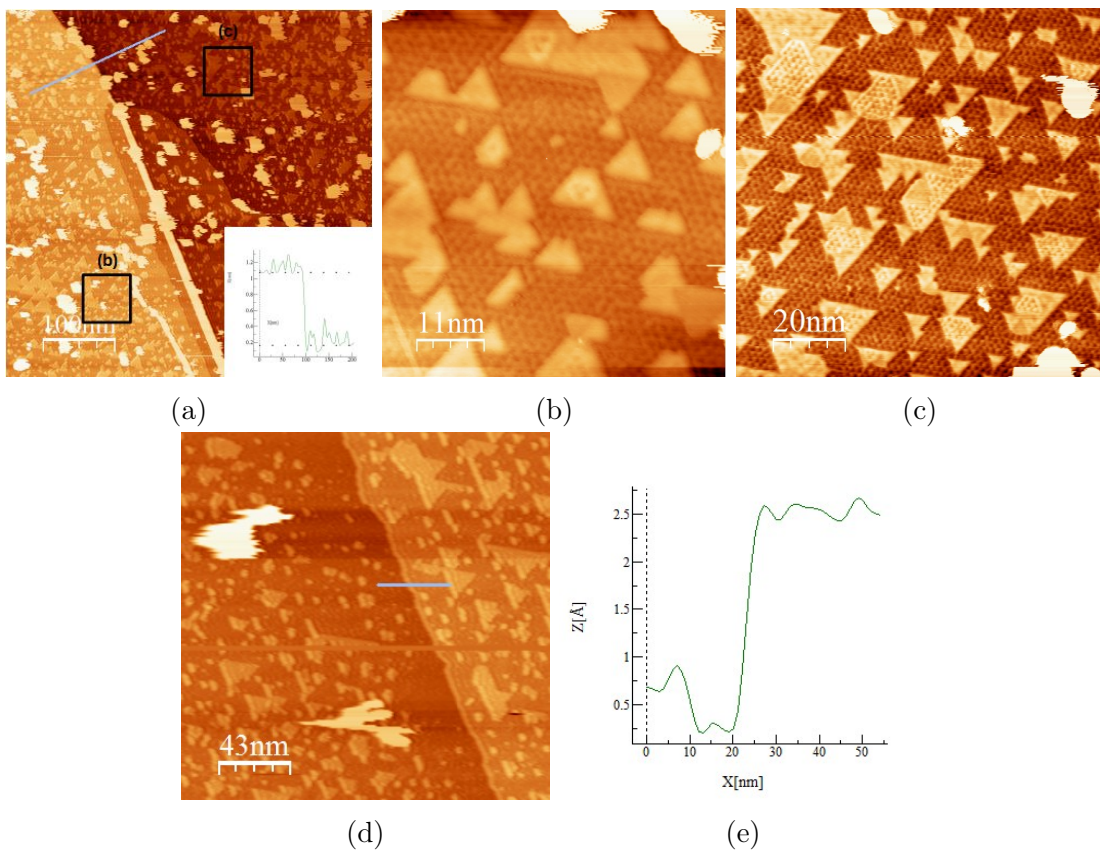


Figure 23: Image parameters of figure (a), (b), (c): 300mV 170pA (a) $500 \times 500 \text{ nm}^2$ scan area (b) zoom on left part of figure (a) $55 \times 55 \text{ nm}^2$ scan area; (c) zoom on the right part of figure (a) $100 \times 100 \text{ nm}^2$ scan area; (d) $215 \times 215 \text{ nm}^2$ scan area; Image parameters: 1V 1nA (e) cross section along blue line in (d)

In contrast, other STM images such as in figure 23d show that bright triangles may be in the same direction between two terraces. The line profile in figure 23e gives an height difference of 2.5 Å, equivalent to one SiC step.

We can wonder why these two configurations coexist. Terraces of 6H SiC can be under different configurations. The first case is when the geometry on the top of SiC is the same between two terraces (figure 24a). In that case, we can suppose that bright triangles between terraces should be in the same direction. The second case is when the geometry on the top of SiC is opposed between two terraces (figure 24b). In that case, direction of bright triangles should be opposed. We can conclude that for a step of 0.25 nm for SiC, both cases are possible. The table 4.1 summarizes what we can expect for different sizes.

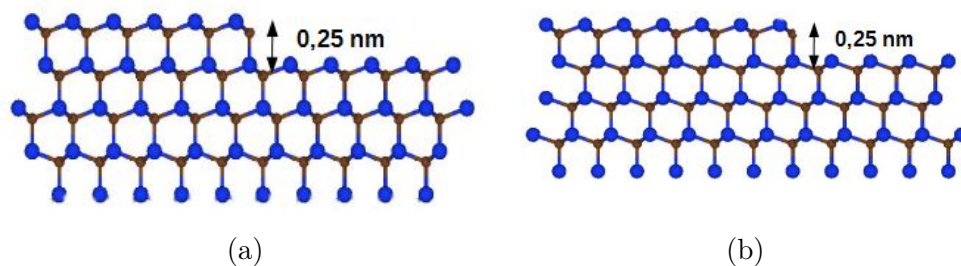


Figure 24: Schema of one step of SiC substrate where geometry of the substrate on the surface is (a) the same (b) opposite

Number of steps	Height difference	Orientation
1	0.25 nm	Both cases possible
2	0.50 nm	Both cases possible
3	0.75 nm	Always opposite
4	1.00 nm	Always opposite
5	1.25 nm	Always opposite
6	1.50 nm	Always the same
7	1.75 nm	Both cases possible
8	2.00 nm	Both cases possible

Table 4.1: Orientation of bright triangles according to the height difference of SiC steps

To confirm these assumptions, different images have been taken as shown in figure 25. No exception was observed after studying 17 images.

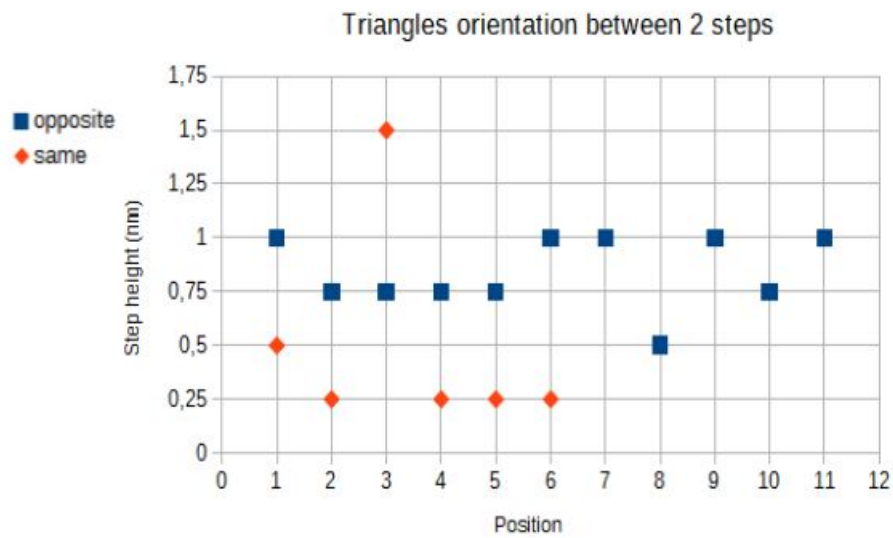


Figure 25: Triangle orientation between two steps at different positions

We can conclude that the orientation of bright triangles between two steps depends on the stacking of SiC substrate.

4.2.3 Dark triangles

By zooming on dark triangle as shown in figure 26b and in figure 26c, we see some big Moiré pattern on the top.

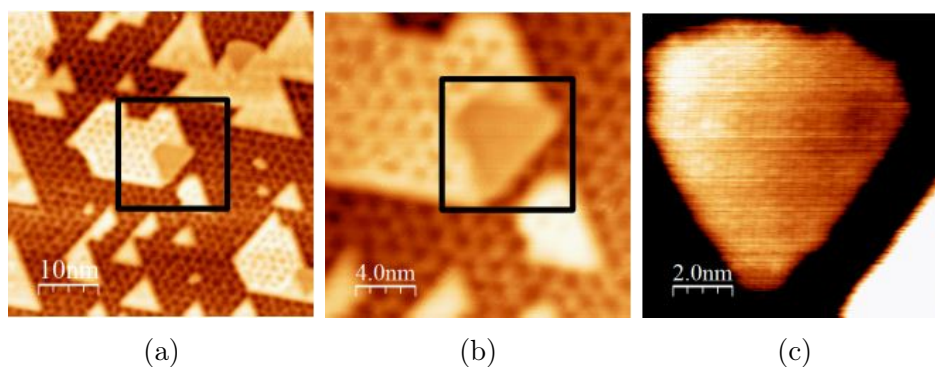


Figure 26: (a) 50x50 nm² scan area; Image parameters of figure: 1V 170pA, (b) 20x20 nm² scan area, Image parameters: 1V 170pA, (c) 10x10 nm² scan area; Image parameters: -1V -170pA

Using WSxM software, the distortion of image in figure 27a is corrected and the result is shown in figure 27b. In this image, three periodicities are observed: a lattice of 0.246 \AA (graphene lattice), a lattice of 0.53 nm and a lattice of 1.7 nm . Moreover, there is an angle of 22° between "1.7 nm" periodicity and graphene zigzag direction. The model which fit with SRM image is that graphene rotate relative to SiC with an angle of 0.73° as shown in model in figure 27c.

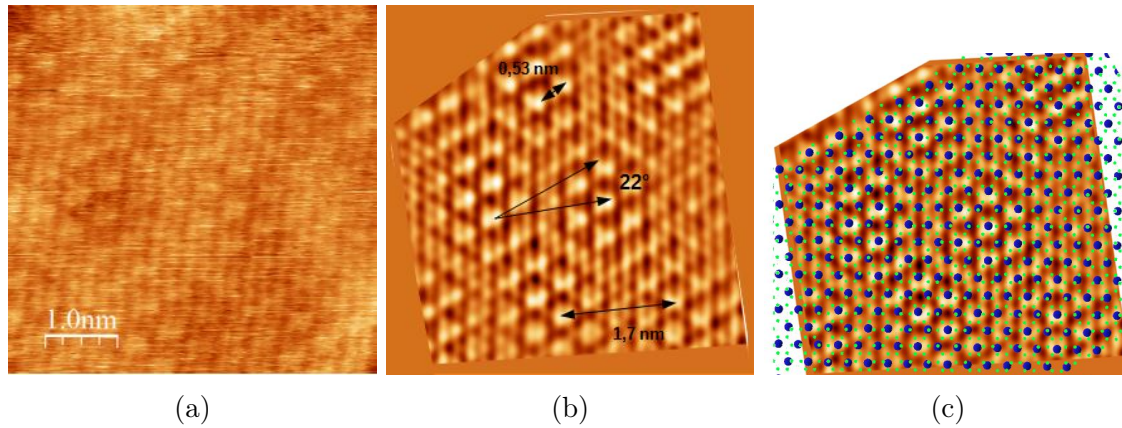


Figure 27: (a) $5 \times 5 \text{ nm}^2$ scan area; Image parameters of figure: -1 V -170 pA , (b) image (a) after correct distortion, (c) model in which there is a rotation of 0.73° between graphene (green circles) and SiC (blue circles)

In this rotated structure, the relationship between Li and graphene is identical at corners of moire cell. Probably the rotated structure has a lower energy than the structure without rotation, or at least they are comparable, nevertheless it requires energy gain due to strain in graphene for rotation. The energy difference is small, so that some Li islands rotate but others do not at high temperature like $6\sqrt{3}$ triangles. But to check this point, more research including energy calculation of the models is needed.

Conclusion

In this report, the Li intercalation and deintercalation in graphene on SiC(0001) have been investigated by STM and LEED.

First, by STM and LEED, changes on the surface after Li intercalation step by step were studied. In particular, Moiré patterns as $(6\sqrt{3} \times 6\sqrt{3})$, 1×1 and $(\sqrt{3} \times \sqrt{3})$ periodicities were observed. Then, Li deintercalation were studied after annealing circles. We saw the growth of $(6\sqrt{3} \times 6\sqrt{3})$ surface and the emergence of new islands with triangle-shaped.

One goal of this work was to study more precisely the height difference between 1×1 and $(6\sqrt{3} \times 6\sqrt{3})$ areas between before and after annealing. According to our experiment, there is no significant difference on buffer layer case contrary to ML case. One explanation of this difference is that Li between buffer layer and ML graphene move between SiC substrate and buffer layer graphene. This model is consistent with S. Fiori's model [9] and with the work of N. Caffrey and L. Johansson [4].

After annealing up to $800 \text{ }^\circ\text{C}$, three different triangle-shaped islands were observed: triangles with 1×1 periodicity, triangles with $6\sqrt{3}$ periodicity and dark triangles. In STM images, the bright triangles always pointed to the same direction. The direction depends on the stacking of SiC substrate. An other question is the nature of the dark triangles. These triangles present three different periodicities. A rotation of graphene relative to SiC substrate of an angle of 0.73 ° could explain these periodicities.

Thanks to this work, more precise data were collected. These data could be useful to build model and to have information for futur devices.

Bibliography

- [1] S. Fiori. *Li functionalized Graphene on Silicon Carbide*. PhD thesis, Universita Di Pisa, 2016.
- [2] G. Capitani, S. Pierro, and G. Tempesta. The 6H-SiC structure model: Further refinement from SCXRD data from a terrestrial moissanite. *American Mineralogist*, 92(403-407), 2007.
- [3] S. Forti and U. Starke. Epitaxial graphene on SiC: from carrier density engineering to quasi-free standing graphene by atomic intercalation. *Journal of Physics D: Applied Physics*, 47(9)(094013), 2014.
- [4] N. Carey, L. Johansson, C. Xia, R. Armiento, I. Abrikosov, and C. Jacobi. Structural and electronic properties of Li intercalated graphene on SiC(0001). *Physical Review*, 93(195421), 2016.
- [5] Bert Voigtländer. *Scanning Probe Microscopy*. springer, 2015.
- [6] E. J. Yoo, J. Kim, E. Hosono, H.S. Zhou, T. Kudo, and I. Honma. Large Reversible Li storage of Graphene Nanosheet Families for Use in Rechargeable Lithium Ion Batteries. *Nano Letters*, 8(2277), 2008.
- [7] E. Rangel, J. M. Ramírez-Arellano, I. Carrillo, and L. F. Magana. Hydrogen adsorption around lithium atoms anchored on graphene vacancies. *International Journal of Hydrogen Energy*, 36(13657), 2011.
- [8] G. Profeta, M. Calandra, and F. Mauri. Phonon-mediated superconductivity in graphene by lithium deposition. *Nature Physics*, 8(131-134), 2012.
- [9] S. Fiori, Y. Murata, S. Veronesi, A. Rossi, C. Coletti, and S. Heun. Li-intercalated graphene on SiC(0001): An STM study. *Physical Review*, 96(125429), 2017.
- [10] J. Emery, B. Detlefs, H. Karmel, L. Nyakiti, D. Gaskill, M. Hersam, J. Zegenhagen, and M. Bedzyk. Chemically Resolved Interface Structure of Epitaxial Graphene on SiC(0001). *Physical Review Letters*, 111(215501), 2013.

- [11] T. Ohta, N. Bartelt, S. Nie, K. Thürmer, and G. Kellogg. Role of carbon surface diffusion on the growth of epitaxial graphene on SiC. *Physical Review*, 81(121411), 2010.
- [12] I. Deretzis and A. La Magna. Role of covalent and metallic intercalation on the electronic properties of epitaxial graphene on SiC(0001). *Istituto per la Microelettronica e Microsistemi (CNR-IMM)*, November 2017.

Appendix A

Experimental conditions

A.1 Sample 1

Degas sample

Voltage (V)	Current (A)	Pressure (mbar)	T Thermo (°C)	T Pyro (°C)	Time
7	0.3	1.8×10^{-9}	360	429	All night
16	0.6	$< 5 \times 10^{-9}$	960	838	All night
19	0.7	$< 3 \times 10^{-9}$	960	954	All night

Table A.1: Experimental conditions of sample's degassing

Li deposition

Pressure (mbar)	Time
$< 8.6 \times 10^{-10}$	1 min
$< 5.2 \times 10^{-10}$	1 min
$< 5.5 \times 10^{-10}$	1 min
$< 5.8 \times 10^{-10}$	10 min
$< 5.8 \times 10^{-10}$	10 min
$< 6.8 \times 10^{-10}$	10 min

Table A.2: Experimental conditions for Li deposition; Parameters: 4.5 V 6.9 A

Annealing

Voltage (V)	Current (A)	Pressure (mbar)	Temperature (°C)	Time
2	0.215	2.8×10^{-10}	150	10 min
7	0.4	$< 2.2 \times 10^{-10}$	400	10 min
9	0.45	$< 2.8 \times 10^{-10}$	505	10 min
11	0.503	$< 2.8 \times 10^{-10}$	600	10 min
16	0.634	$< 2.7 \times 10^{-10}$	798	10 min

Table A.3: Annealing parameters

A.2 Sample 2

Degas sample

Voltage (V)	Current (A)	Pressure (mbar)	T Thermo (°C)	T Pyro (°C)	Time
13	0.4	$< 2.7 \times 10^{-9}$	408	404	All night

Table A.4: Experimental conditions of sample's degassing

Li deposition

Pressure (mbar)	Time
$< 4 \times 10^{-9}$	2 min
$< 4 \times 10^{-9}$	10 min
$< 3.3 \times 10^{-9}$	6 min 20 s

Table A.5: Experimental conditions for Li deposition; Parameters: 4.5 V 6.9 A

Annealing

Voltage (V)	Current (A)	Temperature (°C)	Time
11	0.324	374	10 min
17	0.383	555	10 min
21	0.46	683	10 min
28	0.678	908	10 min












Table A.6: Annealing parameters

Appendix B

Gantt diagram

Expérience échantillon Si: L'échantillon de Si a été étudié grâce à la diffraction d'électrons lents (LEED) et au microscope à effet tunnel (STM) avant et après la déposition du Li.

Expérience échantillon SiC1 et SiC2: Les échantillons ont été étudiés par STM et LEED avant et après la déposition de Li. Puis, les échantillons ont été chauffés à différents paliers puis caractérisés grâce au LEED et au STM.

	Semaine 1	Semaine 2	Semaine 3	Semaine 4	Semaine 5	Semaine 6	Semaine 7	Semaine 8	Semaine 9	Semaine 10	Semaine 11	Semaine 12
Bibliographie												
Prise en main du microscope et autres instruments												
Expériences échantillon Si												
Échantillon vierge												
Déposition Li												
Expériences échantillon SiC 1												
Échantillon vierge												
Déposition Li												
Chauffage												
Trie des données												
Expériences échantillon SiC 1												
Échantillon vierge												
Déposition Li												
Chauffage												
Analyse des résultats	14-mai	21-mai	28-mai	4-juin	11-juin	18-juin	25-juin	2-juil	9-juil	16-juil	23-juil	30-juil

Abstract — This report presents the study of Li intercalation and deintercalation on graphene on SiC substrate by Scanning Tunneling Microscope (STM) and Low Energy Electron Diffraction (LEED). We observed a clear height difference between 1x1 and $(6\sqrt{3}\times 6\sqrt{3})$ areas before and after annealing. Furthermore, triangle-shaped islands with different periodicities appear after annealing up to 800°C. We show that direction of these triangles depends on the stacking of SiC substrate

Résumé — Ce rapport présente l'étude de l'intercalation et la désintercalation du Li dans du graphène déposé sur un substrat de SiC grâce à un microscope à effet tunnel (STM) et à la diffraction d'électrons lents (LEED). On a observé que la hauteur entre les régions avec une périodicité 1x1 et une périodicité $(6\sqrt{3}\times 6\sqrt{3})$ est différente avant et après le chauffage. De plus, des îlots en forme de triangles avec différentes périodicités apparaissent après avoir chauffé au delà de 800°C. On montre que la direction de ces triangles dépend de l'empilement du substrat de SiC.
